

Automated ant scale for annotated image data collection

Department of Bioengineering

Imperial College London

*A Project Report Submitted in
Partial Fulfilment with
Bioengineering Degree*

Word count: 4727

Supervisor: Dr. David Labonte

Department of Bioengineering

d.labonte@imperial.ac.uk

April 2022

Automated ant scale with image data collection

Shihyu Chang, Marcus Iao, Lok Lau, Annie Szeto, Yunyi Wu, Mia Yap

April 13th 2023

Abstract

The efficiency and organisation seen within ant colonies has the power to inspire solutions relating to efficient transport and locomotion. Therefore, the reasoning behind the complex division of labour and varied morphologies seen has been widely sought out. Such studies require large data sets of ant weights to draw accurate conclusions. Current methods of ant weighing require tedious physical removal and often ant death. Therefore, the following paper aims to develop an automated ant-scale and recording setup to gather large amounts of annotated ant weight data without disrupting the ant colony. Experiments were tested on a laboratory colony of *Atta vollenweideri* leafcutter ants and focused on the development of an isolation system, weighing system, and recording framework. Ant detection was achieved via OAK-D cameras used in conjunction with the YOLO detector neural network. The result was a rotating bridge triggered by ant detection, taking images and transporting ants from a 2mm path to a weighing platform based on laboratory-grade open-source scales, adapted to have a higher resolution load cell matching requirements. Results demonstrated a high success rate of isolating individual ants. However, the resultant scale failed to reach the reliability required for 0.1mg precision, instead reaching a 2mg accuracy. Further improvements involve assigning weights with screenshots of ants to generate data sets autonomously. Data collected could be used to train deep neural networks in estimating the weights of ants and their carried plant material from visual input for effortless collection of ant weight data sets of foraging trails.

Acknowledgements:

We would like to thank our supervisors, Dr David Labonte, Fabian Plum, and Dr Natalie Iimirzian, for their guidance and support throughout the project as well as the whole Evolutionary Biomechanics lab at Imperial College London.

1. Introduction

The systematic organisation present in eusocial species has become an increasingly studied topic, with findings inspiring a variety of biomimetic solutions for efficient transport and traffic. Ants in particular have drawn interest as researchers' question, how a decentralised control system is able to methodically organise large groups of individual ants^[1].

Previous ant behaviour research has resulted in the development of ant colony optimisation-inspired computer algorithms (ACOs), used to control large assemblies of robots^[2], find more effective routing solutions to reduce vehicular traffic^[3] or even create optimised factory floorplans^[4]. Current ACOs draw from ant pheromone usage to indicate food sources and foraging paths. However, as Ratnieks highlights in his paper on Pharaoh ant-inspired ACO algorithms^[5], there exist multiple communication mechanisms that remain elusive. Exploring the reasoning behind mechanisms such as their apparent division of labour could potentially improve current ACOs.

Unlike other species, the division of labour present within ant colonies transcends solely reproductive purposes. Sterile ant individuals also show task preferences and morphological differences. This polyethism is best studied in Leafcutter ants, whose colonies are among the most complex and diverse.

Leafcutter ants collaborate to forage for leaf fragments used to grow their fungus farms that act as a primary food source. Therefore, the ability to efficiently harvest and transport leaf fragments is vital for colony survival. Tasks for sterile ants within the colony involve foraging for vegetation, cultivating fungus, defensive efforts against predators and caring for the queen and larvae^{[6][7]}. However, leaf-cutting behaviour specifically is

exhibited by a large spectrum of ants, ranging from 1-30mg (**Appendix C**). This brings into question what role size diversity plays in foraging. Wilson (1980^[7], 1984^[8]) attempted to explain leafcutter ant task specialisation by stating that size variation was due to energy optimisation efforts. Smaller ants require less energy to grow from larvae; however, larger ants are needed to harvest tougher vegetation, concluding that colonies of larger worker ants or increased size diversity have greater efficiency. Recent studies^{[9][10]}, contradict these statements, showing that colony fitness (measured through colony survival, growth, and reproductive success) was unaffected by a decreased worker size diversity. Instead, they suggest that the size of the workforce is more important as ants shift responsibility according to colony needs. With no solid agreement, there is great incentive to understand whether size distribution truly provides any advantage.

Such studies require copious amounts of data regarding ant size to draw reliable conclusions. Current methods of ant size sorting range from freezing ants^{[11][12]} to measuring head widths^[13], requiring manual removal of singular ants per measurement; Both methods cause death or disruption of the colony. Although less precise, people have trained themselves to estimate weights by eye. For example, E. O. Wilson trained himself to estimate ant head-widths by eye^[7], serving as great inspiration for a device that evades colony disruption. Thus, this study aims to create an automated weighing setup to collect large amounts of ant weight data.

To achieve this goal, an automated ant scale consisting of an isolation system, a weighing scale, and a camera setup is proposed. The isolation system will enable automated retrieval by looking at previously researched methods of slowing down and walking speeds^[15] and will transfer of singular ants from foraging trails to the weighing

scale. The weighing scale will then provide an accurate weight for each ant. The addition of a recording setup will provide real-time object detection allowing automation of the isolating system and footage of the ant to be recorded. The output is a large data set of ant footage and their weights.

2. Methods

Designing the automated scale began by researching and developing methods to isolate and weigh the ants separately. Once both designs were functional, a recording setup was put in place, allowing the setup to function without human supervision autonomously.

All firmware used in this project can be found at:
<https://github.com/miayap20/Automated-ant-scale>

2.1 Study animals

Atta vollenweideri leafcutter ants from a colony housed in a climate chamber (FitoClima 12.000 PH, Aralab, Rio de Mouro, Portugal) were used in this study. Ants were kept at 25°C in a 12:12 hour day and night cycle with 60% relative humidity^[13]. Tubing was utilised to create a pathway branching off from paths between the foraging arena and the nest to a testing location.

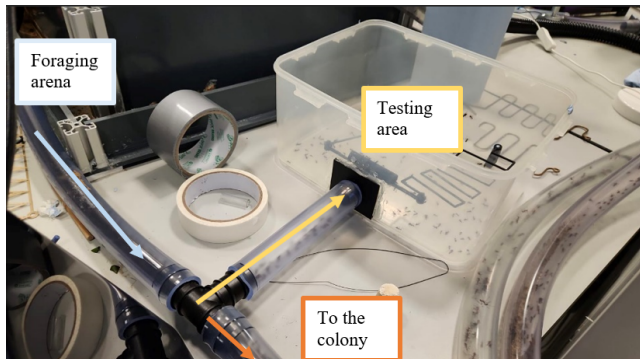


Figure 1- Image showing tube setup from foraging area branching off into our testing area

2.2 Component 1: The Weighing Scale

2.2.1 Design (Appendix F)

The weighing scale required a high resolution for milligram measurements and a

maximum capacity suitable for the required range (**Appendix C**). A high data output frequency was needed to combat mass fluctuations caused by ant movements on the platform (**Appendix F**).

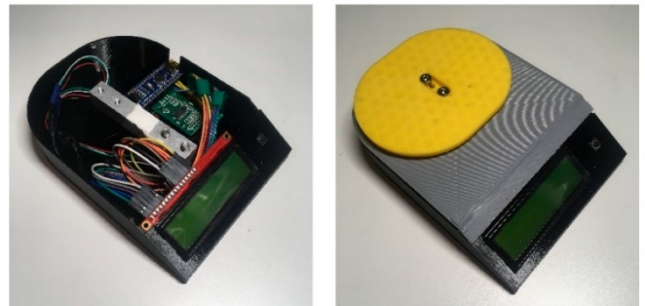


Figure 2 - The Open-Source Digitally Replicable Lab-Grade Scale created by Benjamin R. Hubbard and Joshua M. Pearce

The scale design took inspiration from the *Open-Source Digitally Replicable Lab-Grade Scales* paper by Hubbard and Pearce^[17]. Their scale featured an Arduino circuit, load cell and an LCD, (**fig.2**). Its low-cost base components and modular schematic allowed for much greater control and customisation, serving as the ideal starting point for our design. This was especially important as we needed the flexibility to modify scale components. Having access to an Arduino meant that we could also change the code for future uses such as to implement synced data logging triggered by the camera set-up.

The high-precision load cell used was a strain gauge load cell. In these load cells, an applied force causes the strain gauges to stretch and deform, changing their electrical resistance causing an electrical output signal proportional to the force applied^[18]. The Brans BWSM30 load cell was chosen due to its 1mg precision and 50g maximum capacity which was ideal for measuring ant weights in the milligram range.

The load cell's electrical output was on a millivolt scale. This was too small for accurate detection meaning an amplifier was needed. The HX711 amplifier was chosen as it is universally used, and its calibration code^[19] is widely

available online. Calibration was then necessary to find the factor or function that best describes how the output signal scales from the input force from the load cell.

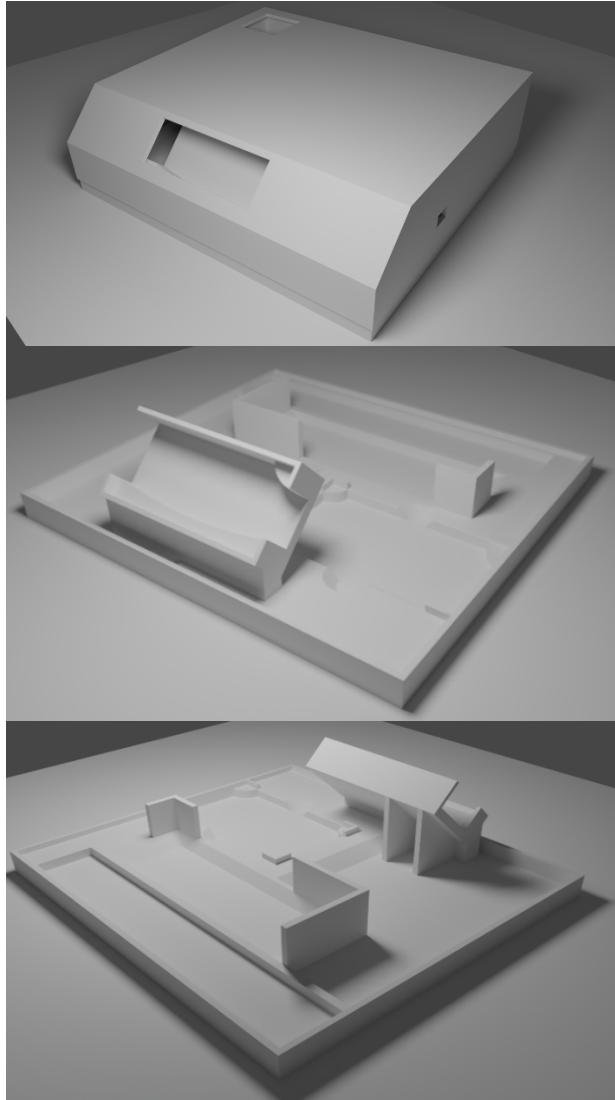


Figure 3 - 3D render of the base of the weighing scale case without the lid using Blender; components were created in SOLIDWORKS before being imported into Blender as STL files and rendered using the Cycles rendering engine. With lid (top), without lid frontside (middle), without lid backside (bottom).

All components used had low power requirements (HX711 having a power range of 2.6V–5.5V, 150mA draw and the LCD a 4.7V–5.3V, with up to 200mA current draw). Hence, a 5V with a 500mA max output mini-USB power supply was

enough to power the circuit through the Arduino. Scale casing was then designed in SOLIDWORKS (**fig.3**) to fully enclose electronics, limiting airflow, which would otherwise affect the amplifier's output.

2.2.2 Assembly

Once a design had been finalised, the electronics were wired according to **fig.4**, based on the circuit design from the DIY Engineers' page^[20]. This schematic used a 1602 LCD which includes an I2C unit, a cleaner alternative that frees up the IO pins on the Arduino, to simplify the circuit wiring.

The functionality of this design was first tested on a solderless breadboard. The main testing focus was on the compatibility of the BWSM30 load cell with the HX711 amplifier, as that had not been tried prior. We wanted to ensure that the amplifier was able to receive signals from this higher-resolution load cell and send them to the LCD to display without loss of resolution.

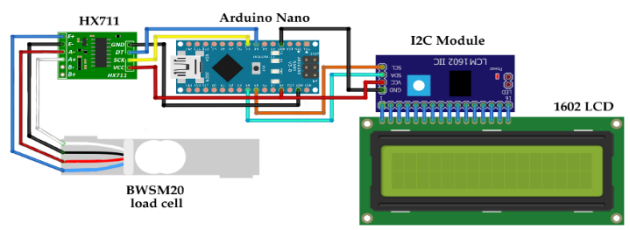


Figure 4 - Weighing Scale wiring of LCD and HX711 with the Brans BWSM30 load cell

To test the HX711 amplifier functionality with the Arduino, a 20kg capacity strain gauge load cell from the Imperial College Electronics Lab was used; the Arduino Nano was connected to a computer with a standard HX711 library for Arduino^[17] via a USB uploaded onto it. The HX711 library included calibration and reading sample codes that utilised the Arduino IDE Serial Monitor to print the load cell's calibration instructions and

mass readings. The BWSM30 was confirmed to have a linear calibration function from the manufacturers. Therefore, calibration entailed an initial tare before placing one object of known mass onto the load cell. After which, the calibration factor was saved onto the Arduino EPROM (Erasable Programmable Read-Only Memory). The `read_loadcell` code was then uploaded, which has the option to read the calibration factor saved onto the EPROM. This meant that recalibration was not necessary every time the load cell was turned on. After testing with 500g, 200g and 100g masses, readings from the circuit were found to be accurate within 10g and it was decided that the HX711 was working correctly. A LiquidCrystalDisplay with an I2C library for Arduino^[19] was then integrated into the firmware such that the reading from the load cell would be printed on the LCD.

COLOURS

Brans BWSM30	Standard LC
E+	Red
E-	Black
S-	White
S+	Green

Figure 5 - Brans wiring colour config configuration VS Standard load cell colours.

After LCD and circuitry functionality was confirmed with the 20kg load cell, the BWSM30 was substituted in. The BWSM30 possessed unique wiring arrangements. A Standard Load cell wiring configuration had red and black wires for E+ and E- respectively, and white and green wires for A- and A+ (signal- and signal+). As shown in **fig.5**, the BWSM30 had a black wire as E-, a blue wire as E+, a white wire as A+, and a red wire as A-. With the correct wiring disposition, the BWSM30 outputted higher resolution readings than the 20kg load cell.

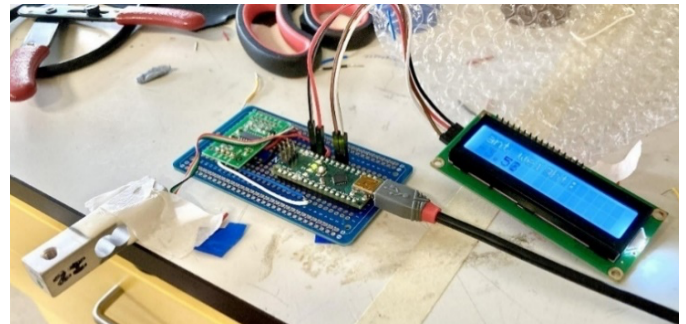


Figure 6 - Testing the soldered circuit with the Imperial College Electronics Lab 20kg load cell.

Components were soldered onto a 52x89mm solder breadboard (**fig.6**). The Arduino was placed at the edge for alignment with the 3D-printed case's hole for USB access. The 3D-printed base contained placeholders to mount the LCD, breadboard, and load cell (**fig.7**)

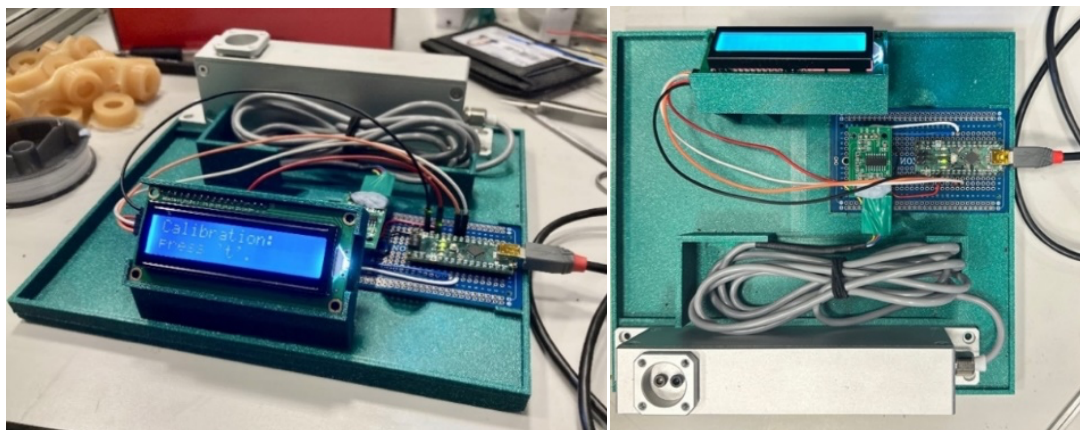


Figure 7 - Weighing scale components fitted onto the 3D printed base. View from the front (left), top view (right)

2.3 Component 2: Ant Isolation System

The second main component was the ant isolation system. The ideal isolation system would separate an ant from high-traffic foraging trails and direct it onto the weighing setup.

2.3.1 Experimental setup:

All experiments were tested in a plastic box of dimensions 30x20x15cm, containing two 32mm diameter holes. These holes allowed the box to connect to the foraging arena via tubing (*fig.8*). Here, a tube is connected to the T-shaped connector that joins the nest and the foraging arena, serving as an entrance and exit for foragers. Paraffin wax was applied to the sides of the container to prevent ant escape.

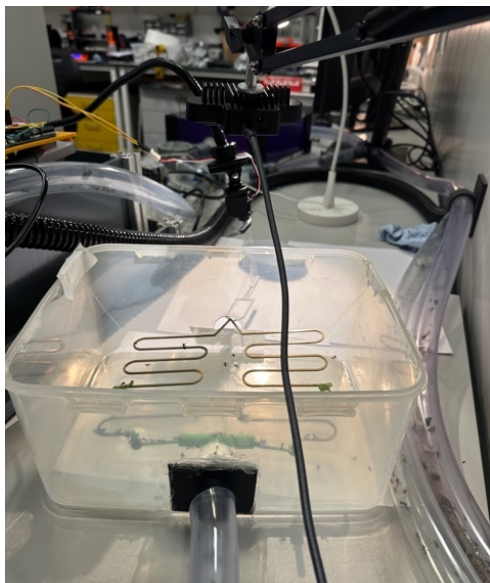


Figure 8 - Experimental Setup in a 30x20x15cm box, connected between the foraging arena and nest via tubing.

Each isolation method was carried out over a period of 45 minutes. 15 minutes were allocated for ant exploration and laying down pheromones to attract a continuous stream of ants. The remaining 30 minutes were used to test idea viability.

2.3.2 Design:

Drawing inspiration from a similar project looking at slowing down ant traffic (Melissa Tan), we chose to utilise narrow paths, reducing the surface area available for ant traffic. Preliminary results showed this reduced traffic to a maximum of 2-3 ants walking side-by-side per path section.

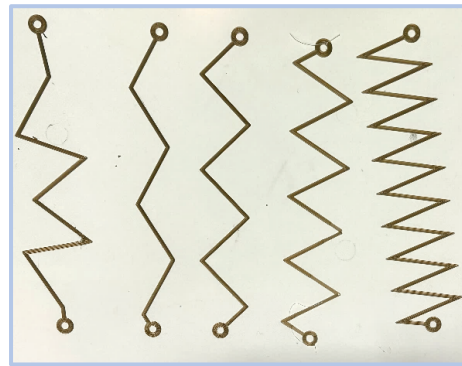


Figure 9 - 2nd stage of path design. 2mm wide paths with triangular edges and circular attachment points at each end. From left to right: Random combination of angles, 120°, 90°, 60°, 30°.

With this knowledge, different path shapes were investigated to maximise path lengths and evenly distribute ants along the paths, avoiding crowding and simplifying isolation. Using the iterative design ability that 3-D printing provides, 2 mm thick triangular-edged paths with angles of 30°, 60°, 90° and 120° were tested (*fig.9*).

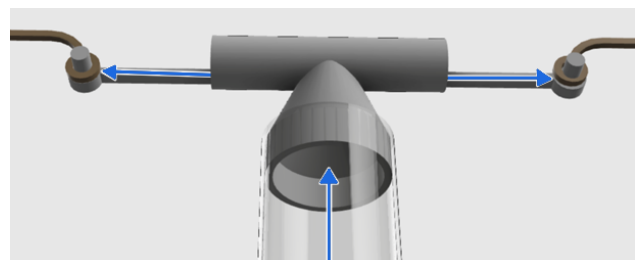


Figure 10 - The tube connector design connecting to the tubing from the foraging trails. Also shows points of attachment for path interchangeability. Blue arrows show directions of ant traffic.

A tube connector was designed to connect to the tubing that branched off existing laboratory foraging trails and contained a straight path with extruded cylinders on its ends (*fig.10*). Circular

ends were added onto the ends of the printed paths to be slid over the extruded cylinders and allow for easy attachment and interchangeability of path shapes for different experiments. Ants exited paths via pieces of cardboard that acted as exit ramps (**fig.11**).

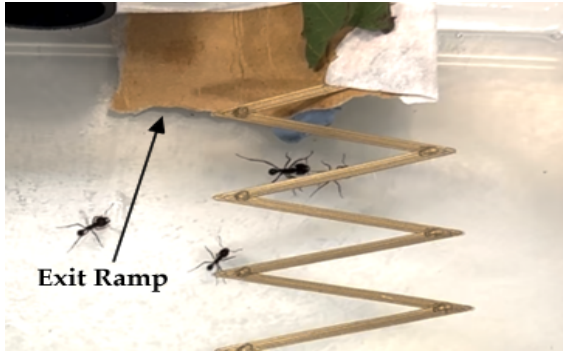


Figure 11 - Sample of a cardboard exit ramp used to enable ants to alight from paths used to test isolation methods.

Observations revealed that if the angle was too small, ants could crawl over the gaps, defeating the purpose of extending path length. Sharp edges discouraged ant movement, leading to the preference for paths with rounded or square edges (**fig.12**). Numerical results and images for rounded paths can be found in **Appendix B**. Summarised, the path in **fig.12a** had the lowest average ants/metre, however, no ants reached the exit ramp. The path in (**fig.12b**) allowed for the same crawling over edges seen in triangular paths with small angles and had a higher, more clumped ant distribution. The most successful path (**fig.12c**) was selected for future work as there was a more even distribution of ants and had the lowest average number of ants/metre where ants traversed the entire path (24 ants/meter) without allowing ants to skip sections of the path.

Thinner paths were also tested but proved too mechanically unstable, deterring ant traffic entirely.

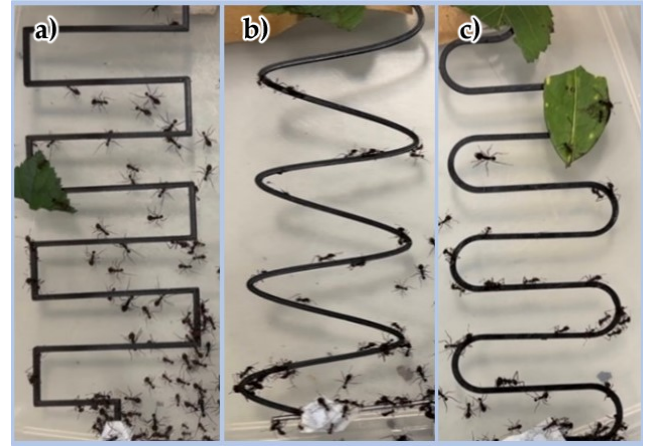


Figure 12 - 3rd iteration of paths. Variations of 2mm wide paths with rounded or square edges were tested for ability to reduce ant traffic. Right path performed the best

With a means of slowing down ant traffic, we began the design of a motor component to move ants from a lower ant density path onto the weighing setup.

At this stage, a 0-10kW potentiometer (**fig.13**) was used to control rotation manually.

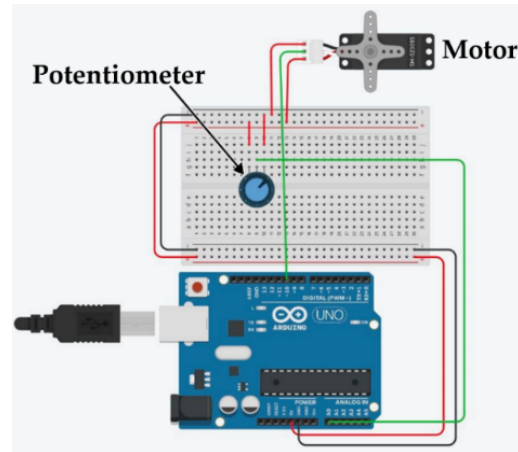


Figure 13 - Circuit diagram of Arduino-motor circuit. Arduino Uno is connected to a potentiometer and motor. Potentiometer value changes lead to rotation in the motor bridge used in our ant isolation mechanism.

The bridge was suspended to prevent ant escape and given a pentagonal shape (**fig.14**) with a 2mm outline to encourage ants to step off the bridge onto the weighing system. Preliminary testing suspending the bridge with fishing wire

proved too unstable, had a delayed reaction time and contained significant rotation angle errors.

Ultimately, a glass slide was chosen to connect the bridge to the suspended motor (**fig.15**) as it provided a compatible surface for paraffin application, preventing ant escape. The final bridge was suspended by a LIVIVO® stand attached to a 3D printed mount.

The path was then adapted to interface with the bridge. The final path design (**fig.16**) formed a square loop, with sides identical to **fig.12c**. A loop was chosen to remove the need for exit ramps due to observed ant accumulation and a triangular contact point was added to the front edge, facing the bridge, for easy transferral of ants onto the bridge. The back edge was connected to the custom 3D-printed tube connector. Paths were printed in lighter colours to amplify colour contrasts with ants, aiding ant detection.

At this stage, the tube connector was also made to have a thicker straight edge for added structural stability and a larger hole diameter to avoid deterring larger ants from entering the setup. The whole isolation setup is shown in **fig.17**.

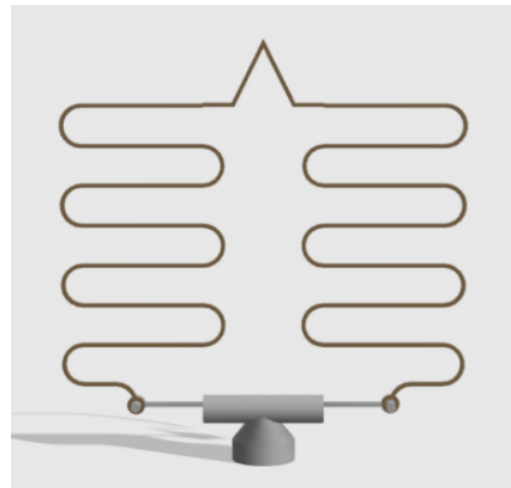


Figure 16 - Top view of tube connector (grey) attached to the final path (gold) used as an ant isolation mechanism. Tube connectors to attach to tubes from foraging trails to lead them to ant isolation testing setup



Figure 14 - Pentagonal shaped bridge attached to a motor used in the ant isolation mechanism.



Figure 15 - Diagrams of the suspended motor setup used to prevent ant escape.
Left: 3D render of an isolated ant moving onto the motor bridge setup
Right: Real footage of an ant attempting to walk onto the motor bridge. Shows the motor bridge connected to a glass slide and a suspended motor.

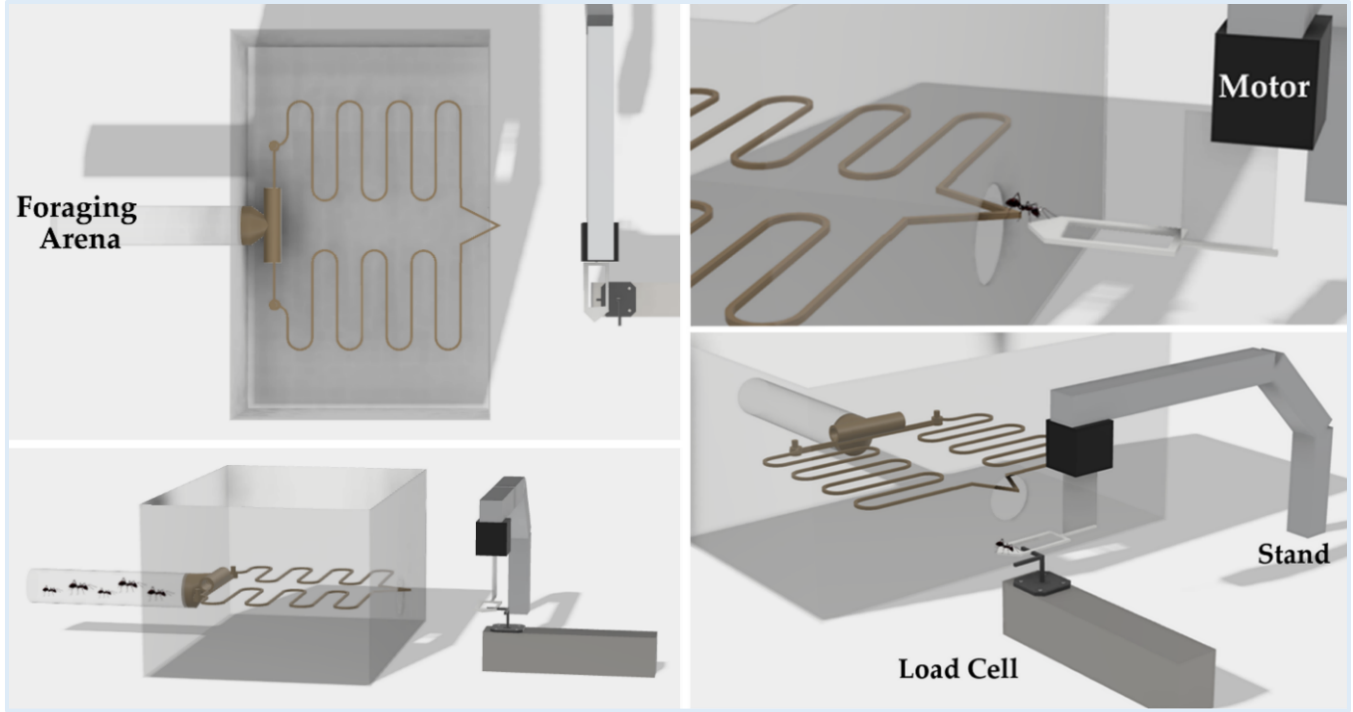


Figure 13 - Multi-angle view of 3D CAD rendering of the ant isolation system design.

Top left: The top view of the setup and tube from the foraging arena, leading to the ant path and tube connector. (gold) in a plastic box. The motor is at 90° setup attached to a stand.

Top Right: 3D render of an ant approaching the motor bridge.

Bottom Left: 3D render of the entire setup.

Bottom Right: Zoomed-in image of load cell and motor bridge interaction.

2.3.3 Camera Setup (**fig.11**)

The final step was to automate the isolation process. Our plan was to achieve this via a camera setup.

First, the use of OAK-D camera with a MacBook (**fig.10**) was tested using pre-existing Python code, TheStick^[21], to track ant locomotion. This code used visual input from a camera mounted 25cm vertically from the bridge and a custom-trained YOLO (You Only Look Once) detector neural network^[16] to track leafcutter ants.

The network used was trained on leafcutter ant data and used a detection-based buffer and recover tracking method. Here each frame was checked for detections by the trained network and was assigned to an active track,

determined using a 2D Kalman filter to extrapolate the track's motion and the hungarian matching method to assign by distance cost.

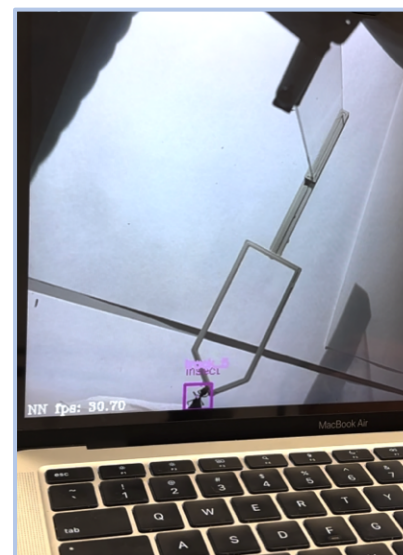


Figure 14 - The display on the MacBook when running THE_STICK_YOLO.py



Figure 15 - Image of the setup used to test the recording setup functionality featuring the testing set up box and a camera mounted on a stand. A placeholder (in grey) was placed to represent where the load cell would be located.

Fig.20 shows different scripts and how they communicated with each other within our setup. We modified the `tracker.py` script to include a Boolean property, `self.ant_presence`, in the `Tracker` class object. Its value was “False” when no ant tracks were detected and “True” otherwise. This property was then passed to `THE_STICK_YOLO.py` and sent to the Arduino UNO via the `pyserial` module^[22]. Previous motor Arduino IDE code was modified have a resting position of 0° , changing to 45° when `self.ant_presence` equalled “True”.

An additional screenshot function was added to capture an image of each ant as they entered the bridge for later use. The `Pyautogui` module^[23] was imported and used the `trackIdCount` property in `tracker.py`’s `Tracker` class object to trigger the screenshot function, ensuring the code would take one screenshot per track.

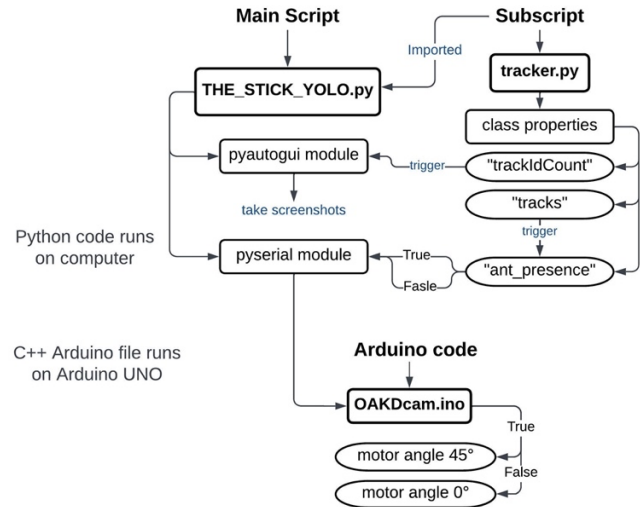


Figure 16 - Flowchart depicting how the different code scripts communicate with each other.

With this, the isolating system was complete. Ants entered the setup, were slowed down by the narrow path, eventually reaching the contact point. An OAK-D camera was positioned to have a view of the bridge and rotated the bridge 45° to the weighing platform when upon ant detection.

3. Results

Akin to the design process, the weighing and ant isolation systems were tested separately to examine individual efficacies.

3.1 Weighing scale

The weighing scale was tested against an analytical lab scale (Ohaus Explorer Analytical Balance EX124) for accuracy.

The scale was first calibrated with a 40019.2mg mass (method in **2.2.2**) and tared. Calibration weights were measured by the Ohaus scale and our scale. A zero-reading after offloading was recorded after 30 seconds (**Appendix B**).

As observed in **fig.21**, the offset (difference between the Ohaus scale and our scale) increased significantly as the mass measured strayed further from the calibration mass. After offloading, it took minutes for the scale's reading to return to its zero-reading state. Readings tend to drift by $\pm 5\text{mg}$ in small masses. Above 5000mg, the response remained linear but was unpredictable below.

The effects of different calibration masses on reading accuracy were further investigated.

The same weights were used to calibrate the weighing scale. They were then removed and loaded again.

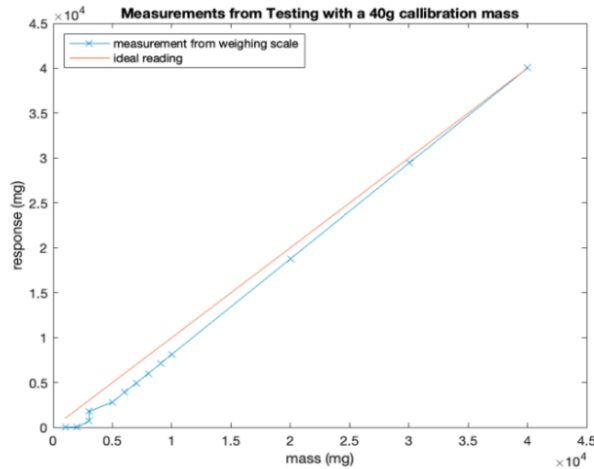


Figure 17 - Graph comparing the readings from the weighing scale with a 40g calibration against the ideal response from a load cell. Recorded values are available in Appendix B.

As shown in **Table 1**, readings became increasingly inaccurate when using smaller calibration masses. A turning point was seen between 5-10g, where fluctuations and drift increased significantly. Below 10g, the offset increased a set amount each time the load was removed or added. The scale was also tested on a vibrationless table and protected from airflow. It was observed that fluctuations decreased for larger masses, however, the inaccuracy of the lower masses persisted.

Calibration Mass (mg)	Weighing Scale Reading (mg)	Initial Zero offset (mg)	Repeated loading (mg)	Repeated zero offset (mg)
40000	40000 \pm 2	0 \pm 1	40000 \pm 2	0 \pm 1
30000	30000 \pm 2	0 \pm 2	30000 \pm 2	0 \pm 2
20000	20000 \pm 2	0 \pm 2	20000 \pm 2	0 \pm 2
10000	10000 \pm 5	0 \pm 5	10000 \pm 5	0 \pm 10
9000	9000 \pm 5	-60 \pm 10	9000 \pm 5	-112 \pm 10
8000	8000 \pm 10	17 \pm 5	8000 \pm 10	20 \pm 5
7000	7000 \pm 5	15 \pm 5	6980 \pm 10	23 \pm 5
6000	6000 \pm 20	60 \pm 10	5980 \pm 20	80 \pm 20
5000	5000 \pm 100	\pm 50	5000 \pm 100	20 \pm 50
1000	1000 \pm 500	\pm 1000	1500 \pm 1000	1000 \pm 1000

Table 1 - Readings from using different Calibration masses. After using a specific mass to calibrate the weighing scale, the mass is cyclically loaded and unloaded without tare, and the readings were observed. In readings from the smaller masses, values tend to drift as time passes, either decreasing or increasing in value incrementally over time with no signs of stopping. After repeated loading, the offset is observed to increase by a factor of the initial zero offsets each time.

Results were consistently accurate with large calibration masses. An intermediary mass (20g) between minimum stable mass (10g) and maximum capacity (50g) was used and tested for small mass detection in a weight range closer to our intended ant targets (**Appendix C**). Small masses of 3.9mg up to 1021mg were procured by cutting strips of wires. The 20g mass was kept on the weighing platform with strips balanced on top.

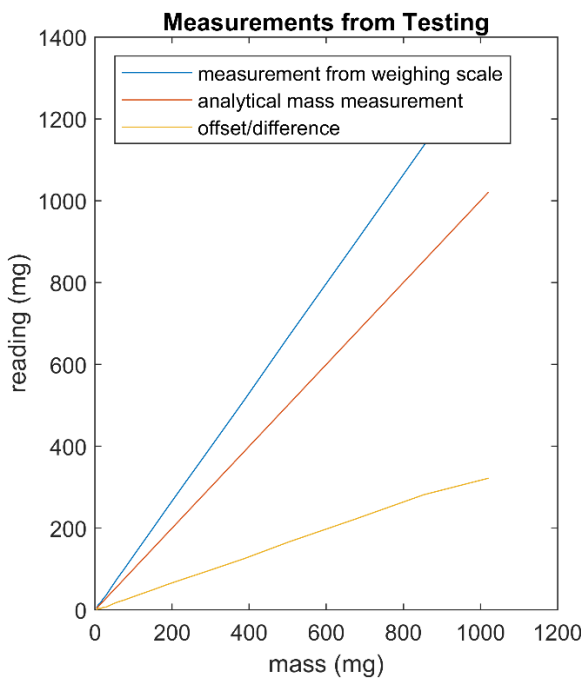


Figure 18 - Graph of the Scale reading, ideal reading, and offset from measuring small masses using a 20g calibration mass. Results table in Appendix B.

From (**fig.22**), the offset of the small masses also scaled linearly against increased mass, which supported the observation from (**fig.21**). This suggested that the offset could be removed using a linear function.

Using MATLAB's polyfit function, we found the correlation coefficients between the weighing scale reading and the associated offset. Using a

20000mg calibration mass and a calibration value of -16.96, the coefficients found were $m=0.694$ and $c=7400.7$ according to the notation of $y = mx + c$ linear relation. The correcting equation was then implemented into the Arduino.

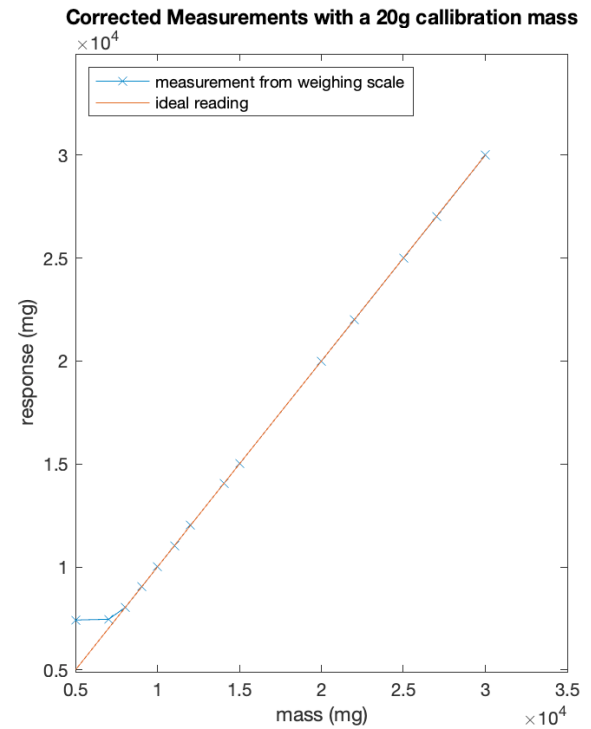


Figure 19 - Corrected Measurements from the Weighing Scale compared with the ideal reading. Results table in Appendix B.

A series of weights from 5-30g were loaded onto the scale with the correction code and measured (**fig.23**). As expected from earlier observations, values below 8000mg did not fit the correction. Readings above 10000mg were decidedly more accurate compared to previous tests, mostly adhering to the ideal reading line.

Using the corrected code, we resumed accuracy testing with smaller weights, repeating the test done for the results in **fig.22** using the correction code in the Arduino, producing **fig.24**.

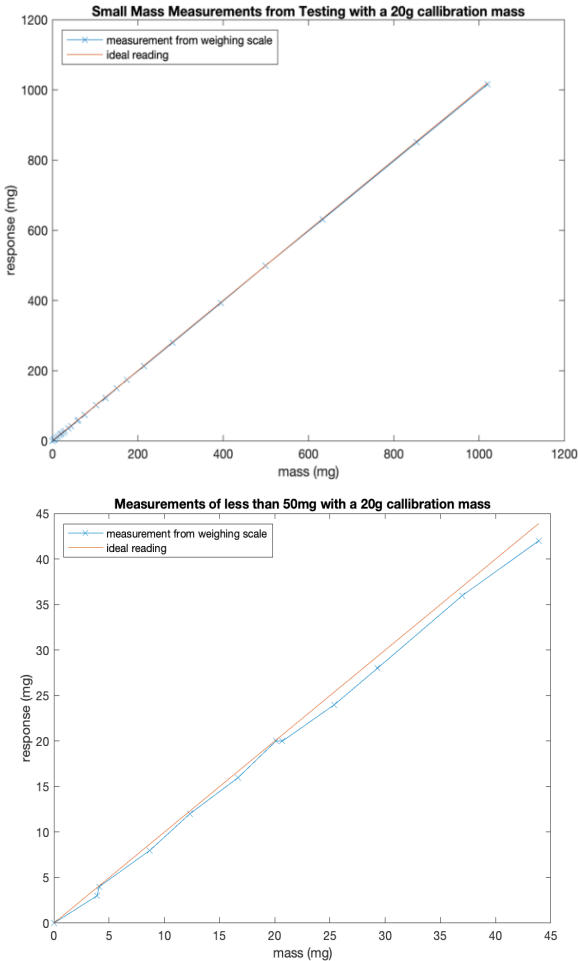


Figure 20 - Results of the corrected readings from the weighing scale using a calibration value of -16.96 and correction coefficients $m = 0.694$ and $c = 7400.7$ for linear correction relation $y=mx+c$. Measurements from around 0-1000 mg (top). Zoomed in results between around 0-50mg (down). Results table in Appendix B

As observed from **fig.23,24**, the offset was minimal after correction. Specifically, for masses less than 500mg (**Appendix B**), the offset was within 2mg, providing a much higher accuracy reading compared to the original result in **fig.22**. However, for masses larger than 500mg, the offset grows, reaching ~ 4 mg offset at over 1000mg.

3.2 Ant Isolating System

The main aims of the isolation system were to extract individual ants from foraging trails without disrupting the colony.

The efficiency of the system of taking an ant from the path to the weighing area was tested in 2 stages. The first tested the success rates of isolating single ants to walk off the path onto the rotating bridge. The second tested success rates of an ant leaving the bridge onto the weighing platform. As this test was a proof-of-concept, a placeholder box modelled the desired location of the scale (**fig.19**).

As before, a 15-minute period was left for path establishment. To activate the camera system, “conda activate depthai” followed by “python THE_STICK_YOLO.py” was entered into the command terminal. The system was run until $n=50$ trials were complete. The 2 success rates mentioned above were recorded (**Table 2**). Once the ant had reached the scale, the ant was removed and placed into a pre-weighed Eppendorf Tube to be weighed on the Ohaus scale. Weights were recorded for further data analysis. Overall performance observations were noted. Full results are in **Appendix D**.

Section of the isolating system being tested	Total number of trials	No. of successful trials	% Success
Path → Bridge	55	49	89.1%
Bridge → Weighing platform	49	42	85.7%
Path → Weighing platform	55	42	76.3%

Table 2 – Results from ant isolation system trials. A total of 5 individual ants were tested and success rates for each mechanism are stated.

Main observations noticed the ant path working optimally, allowing a maximum of 2 ants per section of the path. All failed path-to-bridge transitions arose from fast motor speeds causing

ants to detach. 3 of the 55 trials picked up 2 ants instead of one but number of ants never exceeded 2.

We then checked ant weight distribution. As this project aims to accurately measure all forager ant weights, a concern with the isolation method was that it may be biased against certain ant sizes. We measured a random sample of $n=50$ ants in the laboratory foraging arena to look at their size distribution (**Appendix C**). We then used the sample of 35 ants observed in our setup and compared distributions (**fig.25**). The weights were first tested for normality, and then tested against a significance level at $\alpha=0.05$.

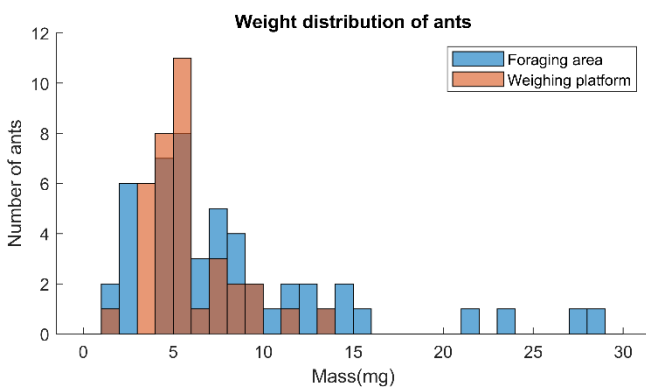


Figure 21 – Histogram of weight distribution of randomly selected ants in the foraging area ($n=50$) (Blue) and ants on the weighing platform($n=35$) (Orange).

Performing a Shapiro-Wilk using a null hypothesis that the weights are normally distributed was set. The P values were all below alpha of 0.05, thus the assumption that both distributions of ant weights were normally distributed was rejected (**table 3**). Thus, a non-parametric test was used to analyse the weights.

Weight Dataset	Shapiro Wilk Test		Wilcoxon Rank-Sum Test	
	P-value	Reject H0	P-value	Reject H0
Colony	1.29e-05	Yes	0.0445	Yes
Sample	0.0012	Yes		

Table 2 - Results of statistical analysis of the distribution of ant weights of the colony in the foraging area and those reaching the platform. P-value and if the null hypothesis is rejected.

A Wilcoxon Rank-Sum Test was performed to test if the test sample mean was significantly different to the colony sample mean. A null hypothesis that the mean ranks of the two samples were equal was used. Tests yielded a p-value of 0.0445, thus we rejected the null hypothesis and concluded with 95% certainty that there was a significant difference between the means of the two samples. This suggested that the ants tested were not representative of the foraging ant population.

4. Discussion

This project aimed to produce an automated, low-cost weighing system to collect large amounts of ant weight data. The result was a weighing setup and an isolation system. Highlighted below are specific outcomes aimed to achieve in this study.

4.1 Weighing Scale Precision

The BWSM30 could measure masses with up to 1mg precision, demonstrated by the manufacturers during their testing. However, this precision was not replicated in this study. Although the load cell has a linear calibration function, the offset of measurements increased as the mass measured strayed further from the calibration mass. Results showed that the load cell became significantly inaccurate when measuring masses of less than 10g, even after testing under ideal conditions on a vibrationless table and with minimal airflow. After consulting the manufacturers, they suspected that this was due to load cell overload. Tell-tale signs of overload are inconsistent display readings and readings not returning to zero after load removal due to deformation of the load cell itself. This could explain why load cell readings took a few minutes to return to zero after offloading. Due to time constraints, it was impossible to order another high-precision load cell, and this hypothesis was not confirmed.

The relation between the scale reading and the offset produced was found, and a function to adjust the measurements was written such that the resulting reading has an accuracy of 2mg when measuring weights of less than 500mg above the calibration mass.

Subsequent development would involve creating a load cell from strain gauges directly to

eliminate dependence on manufacturers while providing additional control over the circuitry.

As of now, the casing includes indents to keep components in place. Future improvements include the addition of fasteners and screw threads to allow for more secure attachment as most components already contain holes for screw attachment.

4.2 Ant Isolating System

The current ant isolation system demonstrated a 76.3% overall success rate in isolating individual ants from a foraging trail onto a weighing platform, with most issues arising from motor speeds that caused ants to fall off. This issue can be resolved by modifying the delay in the Arduino code.

The system showed promising results, with 94% of ants staying on the topside of the bridge, 89% of singular making it onto the motor and only three instances of picking up 2 ants. Successful trials were conducted 42 times in three hours, indicating a good output rate for producing a large dataset. The tracking system exhibited a loss of tracking ability when positioned at a distance from the weighing platform. To enhance the precision and accuracy of tracking, solutions include the use of multiple OAK-D AI cameras, retraining networks with example annotated footage from our recording setup to improve inference quality or manually changing the focal point settings in the code.

Analysis of weight distribution (**Appendix B**) shows potential bias in ant selection, thus skewing the data set if not corrected. Larger ants have a lower tendency to traverse the thin isolation path and activate the tracking system sooner than smaller ants, increasing the failure rate of them reaching the weighing platform.

Future tests should use thicker paths and find a better vantage point.

Future designs should also reduce the need for human intervention. Recommendations include implementing a one-way system for ants leaving the weighing platform, an automatic dropper for dispensing honey water, and a water moat or anti-slip^[24] paint to discourage escape and replace the need for continuous reapplication of paraffin oil. Additional components, such as diffuse lighting to remove harsh shadows and a matte white background, could also facilitate improved ant detection.

4.3 Data collection

It was identified that the rotating bridge used during ant isolation moved too quickly for the camera tracking, resulting in the camera creating two tracks for the same ant and the auto-screenshot function taking multiple images per ant. Even when the motor was stationary, the camera would lose focus on smaller ants. Refining the system to reduce motor speeds and use a multi-camera array for improved lens focus would solve previously stated issues.

The current weighing scale does not record the measured weights. Improvements would be to link camera detection to the weighing scale to trigger data logging for a specific ant and to code a function to measure the average weight of the ant over time so that the incremental fluctuations arising from ant movements can be mitigated. A cloud storage can be opened that would store the photo of the ant as well as the mass measured for convenience. This way, the data could be accessed on non-local devices.

4.4 Cost of Build

A list of parts and the bill of materials can be seen in **Appendix E**. In total, weighing setup parts totalled approximately £290. In comparison, the cost of existing 1mg resolution weighing scales ranges from £88-£1130^{[25][26]}, with scales not being readily adaptable to fit our project's needs. 3D-printed parts reduced costs and aided the iterative testing process. All parts except the BWSM30 were readily available in the Imperial College electronics lab, demonstrating that this device works with components from both the UK and the US (shown in the paper). Current ant-isolating devices are not for sale; therefore, price comparisons cannot be made. However, the device's total cost is £620 (**Appendix E**), which was within the budget.

4.5 Disruption to the ant colony

The final design does not cause ant death or require individual weighing of the ants. All materials utilised were confirmed to be non-toxic, and any electrical components were isolated from contact with ants to prevent harm. Tests to evaluate the effects of running the setup for extended periods on colony viability can be conducted to verify these claims further.

One limitation of the current system is the lack of an exit strategy for ants to return to the foraging arena, disrupting the colony unless ants are manually moved. To address this, an additional hole could be placed in the plastic box as a route back into the colony, ensuring more natural foraging behaviour.

4.6 Whole Setup

Time constraints meant that the whole system was not tested in series. However, the

results discussed show encouraging results for the future combination of parts leading to a fully automated ant weighing device.

Additional parts such as an external box covering the entire setup to combat possible environmental factors (*fig.25*) and a secure method for ants to return to the colonies could improve future setups. Care would have to be taken to ensure proper ventilation and temperatures and when a secure method of allowing the ants to return to the colony is established, the setup could be run unsupervised allowing for longer trials.

To reduce the number of components necessary, both Arduino codes could be combined and run from a single Arduino. The motor and camera could also be directly attached to the outer box to remove the need for stands. In addition, creating a load cell directly from strain gauges would reduce overall prices significantly.

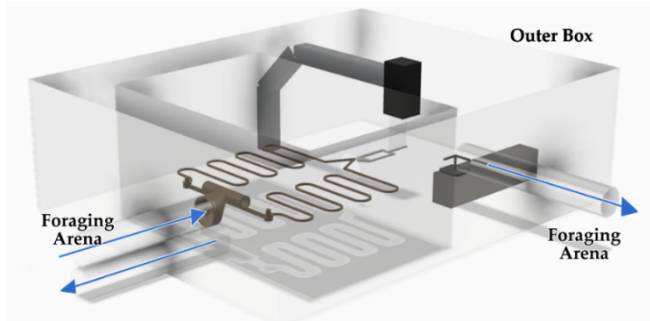


Figure 22 – 3D render of the improved setup with proposed changes added (Outer box and exit strategies)

Conclusion

The basis of this product works as a sound, proof-of-concept for future elaboration. The ant isolating system can track, isolate, and transport an ant to the weighing setup. Future designs should focus on improving the resolution of the weighing platform and developing exit strategies for the ants. When sufficient data has been collected, it can be utilized to train AI networks to identify ant weights from visual input in field settings. In addition, the same setup could be adapted to research other social insect species^[27].

Appendix A

Project management assessment

Acquiring a load cell that fit our high precision demand was more difficult than anticipated. Unforeseen circumstances and issues with the purchasing, shipment and use of the weighing component were the primary sources of delays when producing a final working product according to schedule. An accidental overload of the load cell may have led to permanent damage to the load cell, resulting in inconsistent readings. Faulty wiring configurations provided by the manufacturer impeded the progression to integrating the load cell into our design and resulted in weeks of troubleshooting and part testing.

Difficulties in producing a working weighing scale on time delayed the rest of the project. Testing the combined full setup and methods of transferring the ant from the weighing scale back to the foraging arena and adaptation of both designs to complement one another were impeded. Editing the code to assign recorded weights to images was also postponed due to load cell output issues.

Making full use of lab time

Optimising use of lab time was shown to be an essential project management strategy. It was quickly discovered that testing was the most effective approach for evaluating the viability of ideas when answering questions. We learnt quickly that the best way to answer questions about idea viability was to test. It was crucial to enter the laboratory with well-defined strategies and method protocols to ensure that all group members were aware of the tasks that needed to be accomplished. Drafting of protocols and results tables prior helped us use time in the lab effectively and allowed for full group feedback and tweaking as necessary. Clear logbooks proved useful in keeping track of progress for all group members and finding collaborators within the lab with prior experience was also beneficial timewise as their advice prevented us from carrying out experiments that had already been done.

Prioritising tasks and allocation

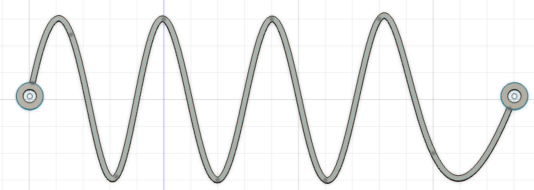
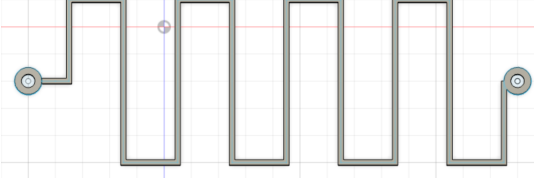
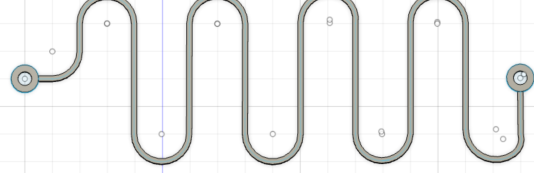
This project contained many working parts, each presenting its own set of challenges. After splitting into two groups (one to work on the scale and the other on the recording system and weighing scale), it would have been beneficial to adapt the people working on either part depending on the situation. For example, the weighing system had unexpected complications which would have benefitted from more minds working on it. Prioritising this component would have allowed earlier identification of issues and ordering of replacement parts that take longer to ship. Likewise, when linking the isolating system and recording setup, time would have been saved if the more experienced programmers had migrated to working on it from the beginning. Instead, clear goals should have been identified from the beginning, with people choosing parts to work on based on their strengths, accompanied by weekly meetings to discuss what had been accomplished for group feedback.

Unpredictability in research projects

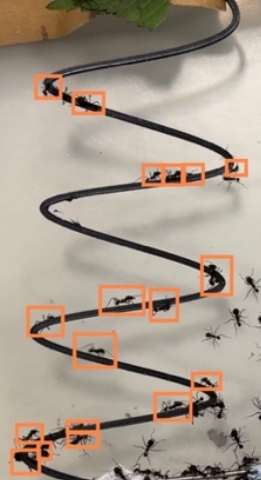
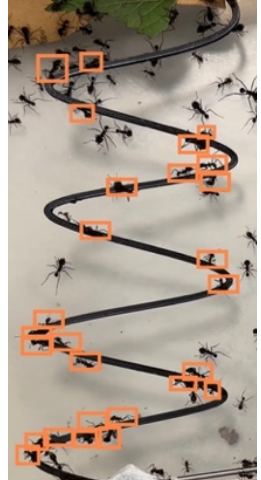
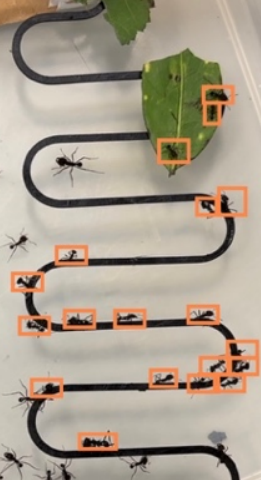
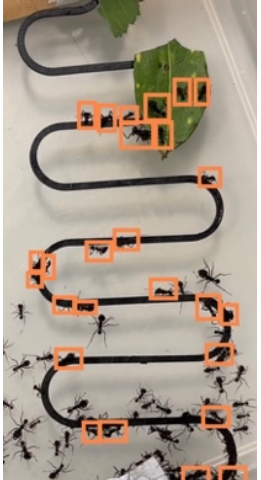
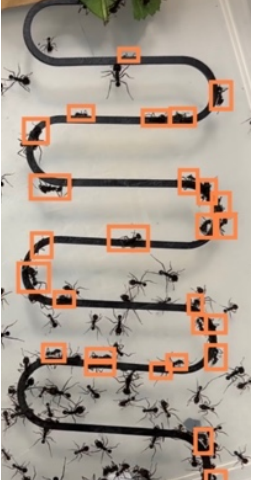
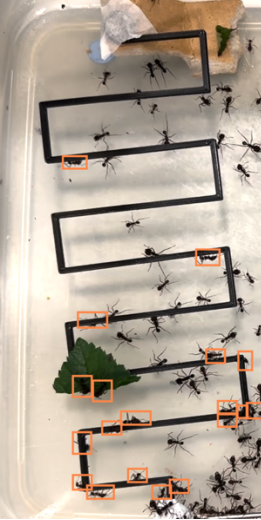
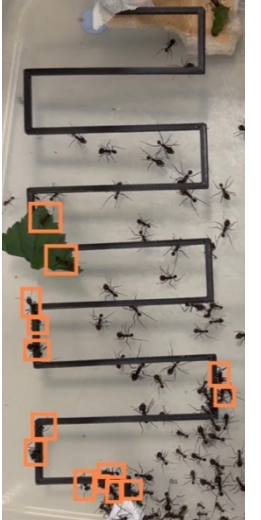
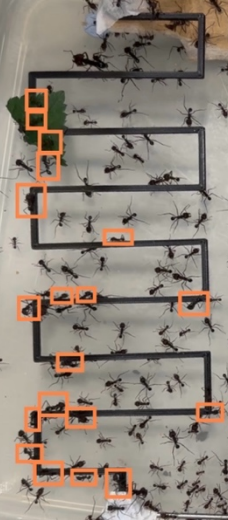
Coping with unpredictability is an inevitable part of research projects. Despite efforts to plan ahead, unforeseen circumstances caused bigger delays than anticipated. For instance, the ordered load cell was delayed due to issues with payment and customs. Furthermore, an accident regarding the load cell may have resulted in irreversible damage caused by applying a force above the load cell's rated capacity. From this, we realised the importance of leaving larger time margins for each stage and having proper communication about handling instructions and precautions to all individuals involved in the project, including non-group members, through the use of labels on the fragile part. The importance of constant communication with supervisors and manufacturers was also highlighted. More frequent contact and guidance enabled us to progress faster, improve pieces of work and simplify the identification of issues, for example, when the load cell manual contained false wiring configurations.

Appendix B

ANT ISOLATING SYSTEM PATH TESTS

Path shape	Time after 15 minutes (minutes)	No. of ants	No. of ants per unit length	Observations
 <p>Total length: 538.543mm</p>	0	18	33.424	Ants can bridge the gap and avoid walking around the edges.
	10	27	50.135	
	20	42	77.988	
	30	30	55.706	
	Average	29.25	54.313	
 <p>Total length: 670mm</p>	0	19	28.358	Overall experiment took too much time. Getting an ant onto the platform may not be feasible with this design. Could work in a design with less time constraints. There was also an uneven distribution with clumping at the corners.
	10	14	20.896	
	20	20	29.851	
	30	19	28.358	
	Average	18	26.866	
 <p>Total length: 788.206mm</p>	0	19	25.258	Even spread out of ants. It was not difficult to incentivise ants onto the path. Even distribution of ants along the paths.
	10	26	38.806	
	20	27	40.299	
	30	24	35.821	
	Average	24	35.821	

Analysed images for the above table. Orange squares show location of ants along the path.

Path shape	Times (minutes)			
	0	10	20	30
1				
2				
3				

ANT WEIGHING SCALE TEST RESULTS

Analytical Lab Scale reading (mg)	Weighing Scale reading (mg)	
Mass measured	Mass measured	"Zero" reading after mass is removed
40019.2	40033	-2
30035.0	29461	-7
20013.6	18771	-6
10017.5	8152	-8
9049.4	7117	4
8047.2	6029	-5
7028.8	4960	-7
6028.8	3924	0
5016.0	2829	-6
4033.4	1786	-4
3037.9	725	-5
2014.7	32	-3
1021.8	2	-7

Table 3 - Comparison of readings of different masses between an Analytical Lab Scale and our self-made Weighing Scale with 40g calibration mass.

Lab Scale reading (mg)	Weighing Scale reading (mg)	Corrected Weighing Scale reading (mg)	Difference (mg)
3.9	20004±1	4±1	0.1
8.7	20013±1	13±1	4.3
12.6	20016±1	16±1	3.4
16.1	20020±1	20±1	3.9
20.1	20026±1	20±1	5.9
28.9	20036±1	36±1	7.1
43.5	20057±1	57±1	13.5
58.6	20078±1	78±1	19.4
75.0	20099±1	99±1	24.0
107.0	20142±1	142±1	35.0
150.6	20200±1	200±1	49.4
182.5	20243±1	243±1	60.5
233.2	20310±1	310±1	76.8
281.3	20373±1	373±1	91.7
388.9	20515±1	515±1	126.1
502.0	20668±1	668±1	166.0
673.5	20895±1	895±1	221.5
853.3	21135±1	1135±1	281.7
1021.0	21343±1	1343±1	322.0

Table 4 - Comparison of measured masses between the Analytical Lab Scale and our Weighing Scale, and the difference between using a 20g calibration mass. Weighing Scale measurements are obtained by keeping the 20g mass on top of the scale and then adding the small masses on top of the 20g mass.

Lab Scale reading (mg)	Weighing Scale reading (mg)	Difference (mg)
5016.0	7426±1	2410.0±1
7029.4	7465±1	435.6±1
8051.3	8049±1	-2.3±1
9050.0	9042±1	-8.0±1
10017.3	10019±1	1.7±1
11039.4	11031±1	-8.0±1
12029.4	12032±1	2.6±1
14050.9	14052±1	1.1±1
15032.8	15032±1	-0.8±1
20000.0	19997±1	-3.0±1
22013.1	22002±1	-11.1±1
25015.8	25011±1	-4.8±1
27027.4	27012±1	-15.4±1
30017.4	30010±1	-7.4±1

Table 5 - Readings comparing the Lab Reading with the corrected measurements from the Weighing Scale.

Lab Scale reading (mg)	Weighing Scale Reading (mg)		Difference (mg)
	Exact	Corrected	
0.0	19977±1	0±1	0.0±1
3.9	19980±1	3±1	-0.9±1
4.1	19981±1	4±1	-0.1±1
8.7	19985±1	8±1	-0.7±1
12.3	19989±1	12±1	-0.3±1
16.7	19993±1	16±1	-0.7±1
20.1	19997±1	20±1	-0.1±1
20.7	19997±1	20±1	-0.7±1
25.4	20001±1	24±1	-1.4±1
29.3	20005±1	28±1	-1.3±1
37.0	20013±1	36±1	-1.0±1
43.9	20019±1	42±1	-1.9±1
58.6	20034±1	57±1	-1.6±1
60.6	20037±1	60±1	-0.6±1
75.4	20051±1	74±1	-1.4±1
102.2	20079±1	102±1	-0.2±1
124.0	20099±1	122±1	-2.0±
150.6	20127±1	150±1	-0.6±1
174.4	20151±1	174±1	-0.4±1
214.5	20190±1	213±1	-1.5±1
281.7	20257±1	280±1	-1.7±1
394.6	20370±1	393±1	-1.6±1
499.1	20476±1	499±1	-0.1±1
633.2	20608±1	631±1	-2.2±1
853.7	20828±1	851±1	-2.7±1

1019.7	20993±1	1016±1	-3.7±1
--------	---------	--------	--------

Table 6 - Comparison of measured masses between the Analytical Lab Scale and the corrected Weighing Scale, and the difference between using a 20g calibration mass. Weighing Scale measurements are obtained by keeping the 20g mass on top of the scale and then adding the small masses on top of the 20g mass.

Appendix C

MASS OF THE ANTS

No.	Mass/mg								
1	7.6	11	8.8	21	5.2	31	14.8	41	7.6
2	13.0	12	11.2	22	1.9	32	7.3	42	21.8
3	4.3	13	5.4	23	4.2	33	4.4	43	5.4
4	6.1	14	15.6	24	2.1	34	5.3	44	4.3
5	28.9	15	12.5	25	7.4	35	5.8	45	9.8
6	12.8	16	2.6	26	6.9	36	27.2	46	2.6
7	14.6	17	4.5	27	10.2	37	2.3	47	1.8
8	5.9	18	4.0	28	4.6	38	8.9	48	7.2
9	8.7	19	2.2	29	6.8	39	11.5	49	5.7
10	23.2	20	9.3	30	2.4	40	5.1	50	8.7

Table 7 – 50 measured ant weights of randomly selected *Atta vollenweiderie* leaf cutter ants from a laboratory foraging arena. Ants were weighed on an Ohaus Explorer analytical balance to observe the weight distribution of leafcutter ants found in the foraging arena.

We randomly selected 50 ants from the laboratory foraging area and weighed them using the lab scale (Ohaus Explorer Analytical Balance). The mass of the ants ranged from a minimum of 1.8mg to a maximum of 28.9mg, with a **median** mass of **6.85mg** and an **average** mass of **8.48mg**.

Appendix D

ANT ISOLATING SYSTEM TESTING RESULTS

Trial no.	Success onto motor? (Y – yes, N – no)	Position on motor path (T – top, B – bottom)	Success onto scale? (Y – yes, N – no)	More than one ant? (Y – yes)	Analytical scale weight (mg)
1	Y	T	Y		4
2	Y	T	Y		3.3
3	Y	T	Y		7.8
4	Y	T	Y		11.9
5	Y	T	Y		1.9
6	Y	T	Y		3.5
7	Y	T	Y		5.6
8	Y	T	Y		8.4
9	Y	T	Y		5.6
10	Y	T	Y		4
11	Y	T	Y		4.4
12	N	T	N		5.3
13	Y	T	Y		4.5
14	N	T	N	Y, two ants	3.4
15	N	B	N	Y, two ants	13.8
16	Y	T	Y		8.5
17	Y	T	Y		5.3
18	Y	T	Y		9.4
19	Y	T	Y		5.3
20	Y	T	Y		4.6
21	Y	T	Y		4
22	Y	T	Y		3.4
23	Y	T	Y		5
24	Y	T	Y		5.3
25	Y	T	Y		5.2
26	N	T	N		6.4
27	Y	T	Y		3
28	Y	T	Y		3.6
29	Y	T	Y		5.9
30	Y	T	Y		7.1
31	Y	T	Y		4.5

32	Y	T	Y		5.5
33	Y	T	Y		4.5
34	Y	T	Y		5.6
35	Y	T	Y		9
36	Y	T	Y		7.2
37	Y	T	Y		n/a
38	Y	T	Y		n/a
39	Y	T	Y		n/a
40	Y	T	N		n/a
41	Y	T	Y		n/a
42	Y	B	N		n/a
43	Y	T	Y		n/a
44	Y	T	Y		n/a
45	N	T	N	Y, two ants	n/a
46	Y	B	Y		n/a
47	N	Escape	N		n/a
48	Y	T	N		n/a
49	Y	T	N		n/a
50	Y	T	N		n/a
51	Y	T	N		n/a
52	Y	T	Y		n/a
53	Y	T	N		n/a
54	Y	T	Y		n/a
55	Y	T	Y		n/a
Total success	49	51	42	52	

Table 8 – Results from analysis of ant isolation system efficacy. The success rates of transferring an ant from the 2mm to a rotating bridge and then from the rotating bridge to a weighing platform were recorded as well as reasons for system failure to identify possible future improvements for the isolation system. Ants that made it onto the platform were also weighed on the Ohaus analytical scale to test for possible biases against certain ant sizes from entering the setup.

Appendix E

BILL OF MATERIALS

Purchased Parts

Component Name	Number of units	Total cost (£)
<u>Brans BWSM30 load cell</u>	1	255.00
<u>HX711 weighing module & header pin</u>	1	4.99
<u>Arduino Nano</u>	1	18.54
<u>16x2 Liquid CrystalDisplay</u>	1	6.50
<u>USB-A to mini-B USB</u>	1	2.28
<u>Solder breadboard</u>	1	1.86
<u>OAK-D camera</u>	1	251.00
<u>Jumper wire</u>	8	0.46
<u>30*20*20cm Plastic box</u>	1	9.84
<u>Adjustable camera stand</u>	1	8.95
<u>Micro servo motor</u>	1	4.00
<u>Arduino uno</u>	1	34.66
<u>Glass slide</u>	1	0.16
<u>AYIZON Stand</u>	1	23.9
Total	-	622.14

3D printed parts

Component Name	Number of units
Ant Path	1
Weighing scale box	1
Weighing platform	1

Brans BWSM30 Load Cell Schematic

1	2	3	4	5	6																																														
A																																																			
B																																																			
C																																																			
D	<table border="1" style="width: 100%; border-collapse: collapse;"> <tr> <td>电源 Exc (+)</td> <td>Blue(蓝线)</td> <td rowspan="2">编号</td> <td colspan="2">BWSM30-1000</td> <td colspan="2">材料</td> </tr> <tr> <td>电源 Exc (-)</td> <td>Black(黑线)</td> <td colspan="2">BWSM30</td> <td colspan="2">处理</td> </tr> <tr> <td>信号 sig (+)</td> <td>White (白线)</td> <td rowspan="2">批准者</td> <td>设计者</td> <td rowspan="2">数量</td> <td rowspan="2">日期</td> <td rowspan="2">图纸编号</td> </tr> <tr> <td>信号 sig (-)</td> <td>Red (红线)</td> <td>校对者</td> <td>制图者</td> </tr> <tr> <td>屏蔽 Sen (+)</td> <td>\</td> <td colspan="2">BRANS MEASURING & CONTROLLING</td> <td></td> <td></td> <td></td> </tr> <tr> <td>屏蔽 Sen (-)</td> <td>\</td> <td colspan="2"></td> <td></td> <td></td> <td></td> </tr> <tr> <td>屏蔽 Shield</td> <td>Yellow(黄)</td> <td colspan="2"></td> <td></td> <td></td> <td></td> </tr> </table>				电源 Exc (+)	Blue(蓝线)	编号	BWSM30-1000		材料		电源 Exc (-)	Black(黑线)	BWSM30		处理		信号 sig (+)	White (白线)	批准者	设计者	数量	日期	图纸编号	信号 sig (-)	Red (红线)	校对者	制图者	屏蔽 Sen (+)	\	BRANS MEASURING & CONTROLLING					屏蔽 Sen (-)	\						屏蔽 Shield	Yellow(黄)							
电源 Exc (+)	Blue(蓝线)	编号	BWSM30-1000		材料																																														
电源 Exc (-)	Black(黑线)		BWSM30		处理																																														
信号 sig (+)	White (白线)	批准者	设计者	数量	日期	图纸编号																																													
信号 sig (-)	Red (红线)		校对者				制图者																																												
屏蔽 Sen (+)	\	BRANS MEASURING & CONTROLLING																																																	
屏蔽 Sen (-)	\																																																		
屏蔽 Shield	Yellow(黄)																																																		
E	1	2	3	4	5	6																																													
F																																																			
G																																																			
H																																																			
I																																																			
J																																																			
K																																																			
L																																																			
M																																																			
N																																																			
O																																																			
P																																																			
Q																																																			
R																																																			
S																																																			
T																																																			
U																																																			
V																																																			
W																																																			
X																																																			
Y																																																			
Z																																																			

Appendix F

Product Specification Document

Project Name:	Automated ant scale
Date:	08-04-2023
Release Number:	V2

Aspect	Objective	Specification	Test Method
Functionality and Performance	Accurate measurement of ant weights	Resolution of the weighing scale is at least 1mg	Placing known weights from 1 to 100mg on the scale to ensure the real-time readings displayed on the screen with a difference of no more than $\pm 1\text{mg}$.
		Be able to measure ants of different sizes ranging from 1-80mg. The maximum capacity should exceed 100mg to ensure the load cell remains undamaged under large ant weight.	Pick a random selection of 50 ants of different sizes from the laboratory foraging arena. Place them on the scale and cross-check the results with readings from a reliable, existing lab scale.
		Quick and real-time measurements of ants (less than 0.1s)	Measure time between placement of the weight and the outputs on scale, then check whether it is less than 0.1s.
	Display of ant weights	Scale must contain a clear method of displaying recorded weights such as use of an LCD screen or computer interface.	Placing known weights on the scale, and the displayed readings should be updated in real-time and easy to read (ie. Readable from 2 meters).
	Control Ant flow	Slow down ant traffic	Branch off foraging arena setup, observe ant traffic over a period of at least 30 minutes. Compare this result with ant traffic visualised on undisturbed ant foraging trails and test efficiency

		Isolating one ant on the scale at a time with a bridge setup	Test the setup by observing the number of ants on the bridge and whether only one ant is allowed at a time on the scale
	Automation of the isolation system	Camera should allow real-time detection of ants along the motor bridge to control ant flow automatically	Setting the camera, leave the setup untouched. Observe the number of successful attempts at isolating the ants. During testing, the motor bridge should rotate when an ant is approaching the camera's field of view.
	Minimizing disturbance to the ant colony	The system must not cause any harm or disruption to the colony.	Conduct measurements using the automated weighing scale. Monitor and record the weighing process for any disturbances to the ant colony, such as ant death in foraging area and the testing box as well as any changes in foraging patterns.
Size and Weight	Fit in a lab (size)	Dimension within 60*30*20cm	Measure the dimensions and weight using a tape measure and scale to verify the setup meets the standards
	Carried with ease	Under 5kg	
Environmental	No environmental impact	Utilize environmental-friendly materials and 3D printing to minimize the waste generation during manufacturing process	Check for any degradation by-products of materials and reactions to temperature or materials that could cause toxic by-products.
Portability	Quick assembly	Assembly of the whole setup, including the scale, isolation system and the camera should take less than 10 minutes. So it can be easily setup for use in scenarios such as on foraging paths	Assemble and disassemble 3 times to see if it takes under 10 mins on average
	No risk of electrocution	All electrical components encased: no contact with the ants or user, no exposed connections, safe from water spillages	Observe whether there is any exposed electronic/ Check all the wirings safety with a qualified individual such as a lab technician.

Safety & Security	Ant escape-proof	Methods to prevent ant escape are enforced such as use of paraffin oil and a water moat.	After directing the ant into the box, leave it for two hours to see if the ants are able to escape.
	Reliable	Minimal system failures resulting in interruptions during operation, with a target of less than 10% of total operating time	Run the system for at least one hour under normal operating conditions and monitor for any failures or interruptions and record the time.
Life, Reliability and Maintenance	Durable and low maintenance	Components are resistant to wear, the setup only has one moving component (bridge), so it doesn't require frequent replacement. Parts can be replaced separately	Disassemble the most fragile parts (motor from the bridge) and check the functionality after applying repeated rotational movements of the motor bridge.
	Run for extended periods of time	Setup can be used unsupervised for 1-2 hours in the lab (ie. Ant must not escape & the code/system must not malfunction within this period.)	Running the setup for an hour to assess its performance.
	Lifetime	Minimum 3-year lifespan	Check schematics of all materials and parts used to ensure that they all function for that amount of time.
Cost	Cost-effective	The whole setup must be under £900	Create a bill of materials to check price points. Ensure parts are widely available for use. All components are checked against a budget sheet before purchasing.
Legal and Regulatory	Compliance with Intellectual Property Laws	Not infringing upon any patents	Conduct online research and review patent database, there are no similar "Ant isolation system" patents

References

- [1] Burns, D. D. R. et al. (2019) "The costs and benefits of decentralization and centralization of ant colonies," *Behavioral ecology: official journal of the International Society for Behavioral Ecology*, 30(6), pp. 1700–1706. doi: 10.1093/beheco/arz138.
- [2] Zhang, Z. et al. (First 2014) "On swarm intelligence inspired self-organized networking: Its bionic mechanisms, designing principles and optimization approaches," *IEEE Communications Surveys & Tutorials*, 16(1), pp. 513–537. doi: 10.1109/surv.2013.062613.00014.
- [3] Dallmeyer, J. et al. (2015) "Don't go with the ant flow: Ant-inspired traffic routing in urban environments," *Journal of intelligent transportation systems*, 19(1), pp. 78–88. doi: 10.1080/15472450.2014.941758.
- [4] Zeng, X. and Ma, Q. L. (2012) "Ant colony optimization for factory layout," *Advanced materials research*, 591–593, pp. 758–761. doi: 10.4028/www.scientific.net/amr.591-593.758.
- [5] Ratnieks, F. L. W. (2008) "Biomimicry: Further insights from ant colonies?," in *Bio-Inspired Computing and Communication*. Berlin, Heidelberg: Springer Berlin Heidelberg, pp. 58–66.
- [6] Wilson, E. O. (1972) *The insect societies*. London, England: Harvard University Press.
- [7] Wilson, E. O. (1980) "Caste and division of labor in leaf-cutter ants (Hymenoptera: Formicidae: Atta): II. The ergonomic optimization of leaf cutting," *Behavioral ecology and sociobiology*, 7(2), pp. 157–165. doi: 10.1007/bf00299521.
- [8] Wilson, E. O. (1984) "The relation between caste ratios and division of labor in the ant genus Pheidole (Hymenoptera: Formicidae)," *Behavioral ecology and sociobiology*, 16(1), pp. 89–98. doi: 10.1007/bf00293108.
- [9] Honorio, R., Doums, C. and Molet, M. (2020) "Manipulation of worker size diversity does not affect colony fitness under natural conditions in the ant Temnothorax nylanderii," *Behavioral ecology and sociobiology*, 74(8). doi: 10.1007/s00265-020-02885-2.
- [10] Colin, T. et al. (2017) "Decreasing worker size diversity does not affect colony performance during laboratory challenges in the ant Temnothorax nylanderii," *Behavioral ecology and sociobiology*, 71(6). doi: 10.1007/s00265-017-2322-4.
- [11] Gibb, H., Andersson, J. and Johansson, T. (2016) "Foraging loads of red wood ants: Formica aquilonia (Hymenoptera: Formicidae) in relation to tree characteristics and stand age," *PeerJ*, 4(e2049), p. e2049. doi: 10.7717/peerj.2049.
- [12] Chiu, M.-C., Wu, W.-J. and Lai, L.-C. (2020) "Carriers and cutters: size-dependent caste polyethism in the tropical fire ant (*Solenopsis geminata*)," *Bulletin of entomological research*, 110(3), pp. 388–396. doi: 10.1017/S0007485319000750.

- [13] Püffel, F. et al. (2021) "Morphological determinants of bite force capacity in insects: a biomechanical analysis of polymorphic leaf-cutter ants," *Journal of the Royal Society, Interface*, 18(182), p. 20210424. doi: 10.1098/rsif.2021.0424.
- [14] Brown, A. (2016) *EveryDayCook*. New York: Ballantine Books, p. 4.
- [15] Clifton, G. T., Holway, D. and Gravish, N. (2020) "Uneven substrates constrain walking speed in ants through modulation of stride frequency more than stride length," *Royal Society open science*, 7(3), p. 192068. doi: 10.1098/rsos.192068.
- [16] Diwan, T., Anirudh, G. and Tembhurne, J. V. (2023) "Object detection using YOLO: challenges, architectural successors, datasets and applications," *Multimedia tools and applications*, 82(6), pp. 9243–9275. doi: 10.1007/s11042-022-13644-y.
- [17] Hubbard, B. R. and Pearce, J. M. (2020) "Open-source digitally replicable lab-grade scales," *Instruments*, 4(3), p. 18. doi: 10.3390/instruments4030018.
- [18] Gupta, S. V. (2012) "Strain gauge load cells," in *Mass Metrology*. Berlin, Heidelberg: Springer Berlin Heidelberg, pp. 89–119.
- [19] Kallhovd, O. (2017) HX711_ADC: Arduino library for the HX711 24-bit ADC for weight scales.
- [20] HX711 & Load Cell - How to Use (with examples) (2022) DIY Engineers. Available at: <https://www.diyengineers.com/2022/05/19/load-cell-with-hx711-how-to-use-with-examples/> (Accessed: April 3, 2023).
- [21] Plum, F. (2022) *TheStick*. Available at: <https://github.com/FabianPlum/TheStick> (Accessed: April 3, 2023).
- [22] Welcome to pySerial's documentation — pySerial 3.0 documentation (2001) Pythonhosted.org. Available at: <https://pythonhosted.org/pyserial/> (Accessed: April 3, 2023).
- [23] *Welcome to PyAutoGUI's documentation! — PyAutoGUI documentation* (2019) Readthedocs.io. Available at: <https://pyautogui.readthedocs.io/en/latest/> (Accessed: April 9, 2023).
- [24] Féat, A. et al. (2019) "Slippery paints: Eco-friendly coatings that cause ants to slip," *Progress in organic coatings*, 135, pp. 331–344. doi: 10.1016/j.porgcoat.2019.06.004.
- [25] Solid. (2015). 1mg Weighing Scale. [Online] Available at: <https://amzn.to/3K2K2RH>
- [26] Torbal. (2012). AD60 0.001g Magnetic Force Restoration Balance. [Online] Available at: <https://amzn.to/3U3D8QK>
- [27] Ammal, R. A., Pc, S. and Ss, V. (2020) "Termite inspired algorithm for traffic engineering in hybrid software defined networks," *PeerJ. Computer science*, 6(e283), p. e283. doi: 10.7717/peerj-cs.283.